land

MDPI

Article

Mapping an Indicator Species of Sea-Level Rise along the Forest–Marsh Ecotone

Bryanna Norlin [1], Andrew E. Scholl [1], Andrea L. Case [2] and Timothy J. Assal [1,3,*]

[1] Department of Geography, Kent State University, Kent, OH 44242, USA; bnorlin@kent.edu (B.N.); ascholl1@kent.edu (A.E.S.)
[2] Department of Plant Biology, Michigan State University, East Lansing, MI 48824, USA; caseand4@msu.edu
[3] Bureau of Land Management, National Operations Center, Denver, CO 80225, USA
* Correspondence: tassal@kent.edu

Abstract: Atlantic White Cedar (*Chamaecyparis thyoides*) (AWC) anchors a globally threatened ecosystem that is being impacted by climate change, as these trees are vulnerable to hurricane events, sea-level rises, and increasing salinity at the forest–marsh ecotone. In this study, we determined the current amount and distribution of AWC in an area that is experiencing sea-level rises that are higher than the global average rate. We used a combination of a field investigation and aerial photo interpretation to identify known locations of AWC, then integrated Sentinel-1 and 2A satellite data with abiotic variables into a species distribution model. We developed a spectral signature of AWC to aid in our understanding of phenology differences from nearby species groups. The selected model had an out-of-bag error of 7.2%, and 8 of the 11 variables retained in the final model were derived from remotely sensed data, highlighting the importance of including temporal data to exploit divergent phenology. Model predictions were strong in live AWC stands and, accurately, did not predict live AWC in stands that experienced high levels of mortality after Hurricane Sandy. The model presented in this study provides high utility for AWC management and tracking mortality dynamics within stands after disturbances such as hurricanes.

Keywords: species distribution modeling; *Chamaecyparis thyoides*; sea-level rise; ecotone; ghost forests

Citation: Norlin, B.; Scholl, A.E.; Case, A.L.; Assal, T.J. Mapping an Indicator Species of Sea-Level Rise along the Forest–Marsh Ecotone. *Land* **2024**, *13*, 1551. https://doi.org/10.3390/land13101551

Academic Editor: Augusto Pérez-Alberti

Received: 18 August 2024
Revised: 12 September 2024
Accepted: 20 September 2024
Published: 25 September 2024

1. Introduction

The outcomes of climate change (e.g., sea-level rises and increasing storm frequency and intensity) threaten numerous coastal species [1–4]. These threats are especially detrimental to plant species that exist in a narrow range and are sensitive to environmental change. Atlantic White Cedar (referred to as AWC), *Chamaecyparis thyoides* (L.) Britton, Sterns & Poggenb. (Cupressaceae), anchors a globally threatened ecosystem that is being impacted by climate change. These trees are vulnerable to hurricane events, wind-driven water-level fluctuations and salinity, sea-level rises, and drainage ditches designed to lower the water table for agriculture [5]. Collectively, these changes, driven in large part by the climate, are shifting the marsh–forest ecotone [1]. Therefore, in order to better manage and conserve AWC, a species sensitive to sea-level dynamics, more accurate information is needed on the location and condition of live stands. An understanding of ecotone dynamics is critical to understanding the effects of climate change; yet it is these areas of the landscape that pose challenges to species mapping efforts as AWC is interspersed with other types of similar vegetation.

1.1. Coastal Forests and Climate Change

Coastal forests and wetlands provide many ecosystem services, including wildlife habitat, coastal erosion protection, water purification and regulation, nutrient cycling, and recreation [6]. However, coastal forests and wetlands are currently threatened by long-term sea-level rises and increased storm intensity and frequency. The spatial distribution of forested wetland areas appears to be closely related to saltwater intrusion and the occurrence of extreme events that control short-term water levels [7]. Forested wetlands are often dominated by tree communities that are not well adapted to increasing saline conditions [7], causing entire forests in the Mid-Atlantic region (of the United States) to shift in favor of more salt-tolerant species. It can be difficult to estimate the projected changes in these coastal forests because the systems are dynamic [8]. However, ecotones, including the marsh–forest boundary, provide a critical location to study the impact of climate change and extreme events on species residing in ecotones because they are often sensitive to change [2].

Globally, wetlands and coastal forests are at risk from sea-level rises, but wetlands in the Mid-Atlantic region are especially at risk. New Jersey has experienced increased rates of sea-level rises over the past 40 years, with a rate of 0.2 inches/year, which is higher than the global average of 0.1 inch/year [9]. Coastal wetlands will need to migrate in order to compete with sea-level rises; however, inland migration could be blocked by bluffs, development, and shoreline protection structures [10]. Trees and other vegetation within the coastal forests can be killed by tidal flooding and storm surges if they are not flood-tolerant or tolerant to the salinity of the flood waters [3]. The exposure to saltwater can create "ghost forests", areas of standing dead trees [4], which represent the conversion of forest into marsh as those areas become inundated, leaving a patch of dead trees behind [1]. This is driven by sea-level rises as well as disturbance events [7]. Therefore, ghost forests provide evidence of a shifting marsh–forest ecotone and can be used to track the movement of the ecotone boundary over time [11].

Hurricanes and severe storms are a threat to the wetlands and coastal forests in the Mid-Atlantic region of the United States. An estimated 400,000 acres of wetlands were inundated as a result of Hurricane Sandy, a category 3 hurricane that struck in late October 2012 [12]. Hurricane Sandy inundated forested areas by creating breaches in the natural barriers that protect these areas from saltwater intrusion. However, it is challenging to understand the impacts of Hurricane Sandy alone on these forests because there are multiple stressors [13]. After Hurricane Sandy, it was reported that severe degradation occurred in 41.4% of wetlands, and 51.1% of the damage from all types of degradation (including severe, moderate, and low) was long-term damage [6]. Some plant species will be more tolerant to the increased salinity that can be the result of a disturbance event; however, those others unable to adapt will need to migrate or could face widespread mortality due to these increasing threats.

1.2. Atlantic White Cedar Ecosystem Biogeography and Vulnerability

Atlantic White Cedar is a coniferous, evergreen species that is found in the Eastern United States, from Maine to Mississippi, in a narrow band [5], rarely more than 200 km from the coast [14]. AWC generally occurs in narrow belts along streams and can persist seaward to tidal areas where it anchors the forest–marsh ecotone [15]. AWC influences soil characteristics through peat building and provides a habitat for rare and endangered species [5,16,17].

AWC is vulnerable to anthropogenic climate change, which is causing increased storm frequency, intensity, and coastal flooding. The species is salt-intolerant and can experience reduced growth and increased mortality in response to inundation. AWC ghost forests are prevalent in coastal areas of the Mid-Atlantic regions of the US due to increased pressure from sea-level rises [4]. The increase in ghost forests at the marsh–forest ecotone is effectively tracking hotspots of increased salinity and inundation [7,11]. There have been ghost forests further inland in response to periods of inundation [4], and AWC ghost forest formation was reported after Hurricane Sandy in New Jersey [5].

1.3. Predictive Habitat Distribution Modelling

Species distribution models (SDMs) relate species distribution data to the environmental characteristics of an area and have been utilized in diverse environments for a wide variety of species (e.g., Assal et al., 2015, 2021; Hailu et al., 2017; He et al., 2019) [18–21]. SDMs can be used to estimate the potential distribution of a species, then to predict the extent of suitable habitat over a given area [22,23]. SDMs are used to forecast forest species ranges that may be the most impacted by climate change or extreme events, providing valuable knowledge for potential management or mitigation practices [24]. Atlantic White Cedar wetlands are difficult to access due to the surrounding environmental conditions, making it more difficult to monitor these stands [25]. Therefore, an AWC SDM would be beneficial for informing the current and potential areas, as well as identifying areas of the landscape that may be more susceptible to impacts from climate change.

SDMs use environmental data, including both abiotic and biotic variables, to map and predict species occurrence across a landscape. Incorporating remote sensing data into the process, known as predictive habitat distribution modelling [19,26], allows for a more dynamic model because it captures vegetation phenology [27]. Advances in multispectral satellite capabilities provide the opportunity to identify a more complete spectral signature, or response, of a species. A spectral signature is the unique reflectance of a specific material or object over a range of wavelengths [28,29] and aids in discriminating vegetation types and plant stress [30,31]. More recent satellite sensors such as Sentinel-1 (Synthetic Aperture Radar) and Sentinel-2 (multispectral imagery) have been used for vegetation classification and habitat monitoring [32]. The inclusion of both Sentinel satellites in forest mapping has led to higher model accuracy [33]. The combination of remotely sensed and abiotic variables to map and predict species distributions across spatiotemporal scales is a technique that is applicable to many scales and locations due to increases in data availability and computational power.

1.4. Research Questions and Objectives

Understanding AWC distribution will help inform management and mitigation loss strategies associated with climate change impacts. A species distribution model will enable efficient mapping, as AWC grows in wetlands that can be challenging to access. The purpose of this study is to determine the distribution of Atlantic White Cedar throughout southern New Jersey, an area that experienced a severe disturbance, Hurricane Sandy, in 2012. Our primary goal is to create a transferable framework to map the distribution of Atlantic White Cedar and provide managers with the current extent of the range. The main objective of this study is to (A) determine the distribution of AWC throughout southern New Jersey. To help address the primary research goal, there were two smaller research questions addressed: (B) What are the driving predictors of AWC presence across the landscape? (C) What is the spectral signature of Atlantic White Cedar? This research will address a data gap about the distribution of Atlantic White Cedar, provide insight on the vegetation dynamics within these stands of trees, and lead to a better understanding of where AWC is able to persist on the landscape.

2. Materials and Methods

2.1. Study Area

The study domain comprises 36 HUC-12 watersheds (Hydrologic Unit Code (HUC) 12) [34] throughout southern New Jersey that contained known stands of Atlantic White Cedar (Figure 1). This area, 3,430 square kilometers, contains part of the New Jersey Pinelands, which support a wide variety of plant and animal communities that are threatened by water-quality changes and degradation of watersheds from development and agriculture throughout the southern part of the state [35]. Average annual precipitation range is 106.7–116.8 cm, and the average annual temperature is 0–2.2 °C in winter and between 22.2 and 25 °C in the summer months [36]. The pinelands are composed of many different tree species, including pitch pine, red maple, oak tree varieties, and Atlantic White Cedar, which dominates the wetlands areas [36,37].

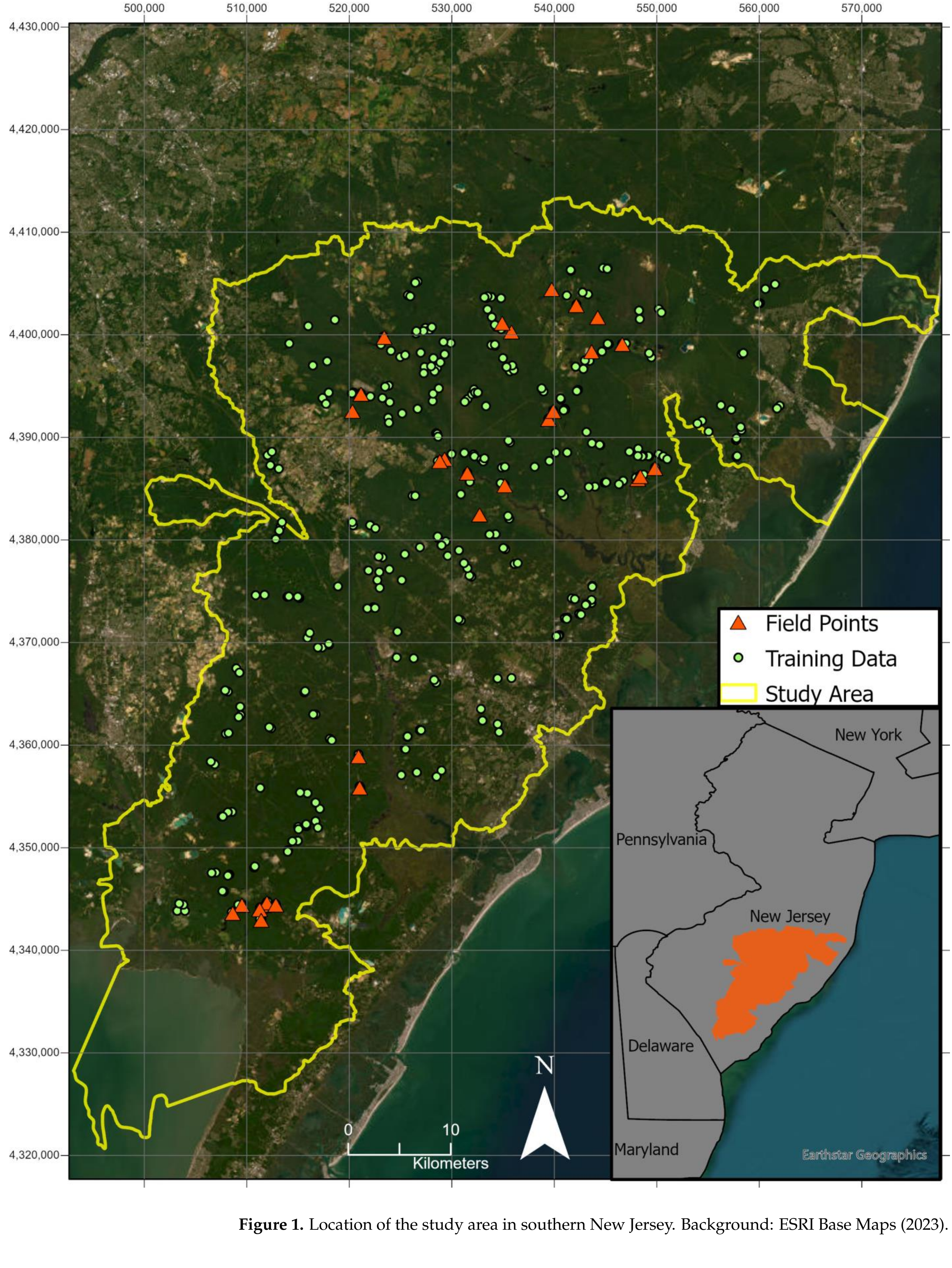

Figure 1. Location of the study area in southern New Jersey. Background: ESRI Base Maps (2023).

2.2. Sample Data Collection

Live and dead AWC stands were documented using a GPS unit (Geode GNSS Receiver; Juniper Systems; Logan, UT, USA) and photographs during a field campaign in August 2022 (Figure 2). Information on the stand condition and setting was documented, including photographs, to provide reference for the position of the stand of AWC during the aerial photograph interpretation process. A total of 30 field sites were visited. The number of stands able to be reached was limited due to the relative inaccessibility of AWC stands on public land (we accessed private lands when permission from the landowner was received) for aerial photograph characterization of AWC. Additional AWC presence points were created through aerial photo interpretation in inaccessible areas.

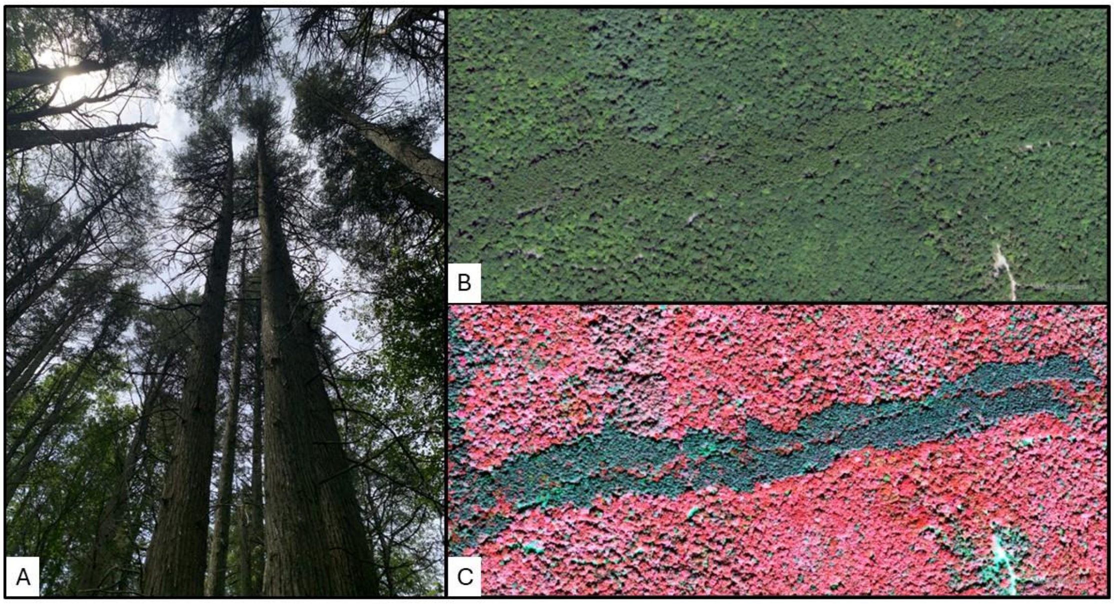

Figure 2. Multiple perspectives of Atlantic White Cedar stands. Panel (**A**)—Field photograph of an AWC stand taken during the 2022 field season. Panel (**B**)—Natural color NAIP imagery showing an AWC stand that was visited during the 2022 field season. Panel (**C**)—Same AWC stand as panel B, shown in color infrared with a contrast stretch applied. AWC is distinguished by its unique texture, tone (the blueish-gray tone), and shape as these stands are typically linear.

Images from the National Agriculture Imagery Program (NAIP) were obtained from the USDA data gateway [38] for the southern New Jersey area. The most recent NAIP photos at the time of analysis were used (26 July–29 September 2019) and had a spatial resolution is 0.6 m in four spectral bands (blue, green, red, and near-infrared (NIR)). The NIR was critical to delineate vegetation from the surrounding environments and distinguish differences in vegetation types (Figure 2). The stands in the field sites served as reference areas for photo interpretation of AWC stands to then develop additional training points (n = 362, 134 AWC presence points, 228 absence points). Contrast stretches were applied to the NAIP imagery to highlight the unique texture and pattern of AWC compared to the surrounding vegetation. This photo interpretation technique has been used previously to develop presence/absence data in SDMs [18–21].

We derived a dataset of mapped AWC polygons from a 2012 Land Use/Land Change (LULC) dataset [39] that had been iteratively updated from the original 1986 dataset created through photo interpretation using a minimum mapping unit of 2.5 acres. This is the only known dataset of mapped AWC in this area, and it was last generated in 2012, just prior to Hurricane Sandy (late October 2012). This afforded an opportunity to compare the pre-hurricane AWC with our updated model and document any change in AWC stands since that time. The LULC data also informed the training dataset using a modified stratified random technique to ensure adequate coverage of vegetation types that may occur near AWC stands. Training points were deterministically placed in six LULC classes: AWC, other coniferous species, water, built/urban, deciduous, and agriculture. Later, additional absence points were added to assist with model training: 10.7% of the training points were water, 12.4% deciduous, 3.0% built environment, 4.4% agriculture, and 18.5% other conifers/pine. More points were placed in areas that may have had more similar characteristics to AWC, such as deciduous and other conifers/pine. After points were classified, the classification scheme was later collapsed to simply AWC presence (1) and absence (0) for use in the random forests model.

2.3. Satellite Data

Remotely sensed variables were derived from Sentinel-1 and Sentinel-2 imagery, as both provide information about stand structure, age, vegetation biophysical parameters, chlorophyll content, leaf area index, aboveground biomass, and more [33,40,41]. We utilized a suite of multispectral bands from the Sentinel-2 surface reflectance (Level 2A) product ("COPERNICUS/S2_SR") in Google Earth Engine (GEE), as well as two derived vegetation indices (Table 1). We acquired imagery during a leaf-on period (15 June–15 September) and a leaf-off period (1 January–15 February and 1–31 December), all during 2021 for consistency (a portion of the study area experienced a wildfire in 2022). We enforced a minimum observation threshold of four clear-sky observations during the leaf-on period for a given pixel to be considered in the analysis; the leaf-off period only required one observation. If a pixel failed to meet the minimum valid observations, it was dropped from the analysis as it could influence the composite image [18]. AWC is a coniferous species that retains needles during the late fall and winter seasons, whereas deciduous vegetation does not retain leaves during that time. We use two time periods as an opportunity to exploit the divergent phenology of AWC from nearby deciduous trees [18,19]. After the minimum observation filter was applied, the mean composite images were exported from GEE for each band and time period (Table 1). We also chose to incorporate the Sentinel-1 C-Band Synthetic Aperture Radar (SAR) ("COPERNICUS/S1_GRD") to account for potential distinct polarization characteristics that coniferous AWC might exhibit over the growth form of deciduous species. We compiled mean composites for the VV and VH band from the same time periods from ascending orbit of the satellite. No minimum observation threshold was applied as SAR is not affected by clouds [33]. Sentinel 2-A bands 5–7, 8A, and 11–12 were resampled from 20 m to 10 m using bilinear interpolation to match the spatial resolution of Sentinel-1 and Sentinel-2-A bands (2–4 and 8) in GEE. All composite bands (Table 1) were exported for further processing in the R statistical software (version R-4.2.2) [42] using the raster package [43].

Table 1. Description of explanatory variables considered in the analysis.

Variable	
	Biotic
VV Band	C-Band SAR vertical transmission/reception
VH Band	C-Band SAR vertical transmission and horizontal reception
Band 2	Blue band
Band 3	Green band
Band 4	Red band
Band 5	Red Edge band 1
Band 6	Red Edge band 2
Band 7	Red Edge band 3
Band 8	Visible and near infrared
Band 8A	Visible and near infrared
Band 11	Shortwave infrared (SWIR)
Band 12	Shortwave infrared (SWIR)
NDVI (Normalized Difference Vegetation Index)	NDVI = (B3 refletance − B2 reflectance)/(B3 reflectance + B2 reflectace) [44]
NDRE (Normalized Difference Red Edge)	NDRE = (B8 reflectance − B6 reflectance)/(B8 reflectance + B6 reflectance) [45]

Table 1. *Cont.*

Variable	
	Abiotic
Percent sand in soil	Percent sand found in soil at a depth of 30–60 cm
Saturated soil water content	Saturated soil water content at a depth of 30–60 cm
Elevation	Derived from DEM
Slope	Derived from DEM
Aspect	Derived from DEM
Topographic Position Index	A measure of slope position and landform type with respect to adjacent grid cells [46]
Topographix Wetness Index	A measure of topographic control on hydrologic processes [47]
Topographic Ruggedness Index	A measure of the elevational difference between a cell and adjacent cells [48]
Northness	Cosine transformation of aspect
Eastness	Sine transformation of aspect
Distance to water	Distance from each cell center to the closest water source
Distance to head of tide	Distance from each cell center to the closest point inland that the tide reaches
Latitude	Latitude at the cell center
Longitude	Longitude at the cell center

Spectral Signatures and Phenology

Spectral signatures of multiple vegetation types were created to determine if the spectral signature of AWC was similar to other vegetation types within the study area, as the inclusion of phenology in SDMs is often overlooked [49], and, to our knowledge, the spectral signature of AWC measured by Sentinel-2A has never been documented. Therefore, we investigated the spectral signature of AWC and other nearby vegetation during the leaf-off and leaf-on periods to aid our understanding of satellite-derived reflectance changes throughout the year in these vegetation types. Spectral responses are influenced by plant physiological traits such as leaf type, chlorophyll content, and water content [31,50]. Coniferous species are known to be more absorptive than deciduous forests and tend to have low values in the near-infrared region [51]. Some vegetation types emit similar spectral responses, and to determine if any of the surrounding vegetation had similar reflectance values in any of the Sentinel-2A bands, the responses for 8 different vegetation types were determined for both the leaf-on and leaf-off periods.

2.4. Topographic and Abiotic Data

We derived a suite of topographic variables from a 10 m digital elevation model (DEM) accessed in GEE ("USGS/3DEP/10m") to be used as predictor variables (Table 1). A new dataset was derived to determine the distance to water using an NJ Coastline dataset [52] and an NHDPlus dataset [34] that provided mapped tributaries, canals, and drainage ditches. The two datasets were intersected in a GIS to create a single dataset representing the coastline, river and tributary banks, and the centerline of smaller streams. Finally, a proximity raster was created that represented the Euclidian distance for each cell to the nearest water source. The distance to the head of tide (HOT), the furthest point inland on any tributary where the tide reaches, was created by calculating the Euclidian distance of each raster cell to the HOT [53]. Given AWC's sensitivity to changing salinities, this was an important variable to consider as vegetation within the tidal zones may be more prone to mortality in the future with an increase in the sea level. We obtained both percent sand and saturated soil water content (at depth of 30 to 60 cm) from the Polaris dataset [54], available through GEE. This depth was chosen based on the root characteristics of AWC, which are shallow and only reach about 0.3–0.6 m [25]. The 30 m data were resampled to 10 m to match the scale of all other covariates using bilinear interpolation.

2.5. Predictive Habitat Distribution Modelling

To relate the presence and absence points to the underlying environmental conditions to be able to predict AWC presence, a random forests (RF) machine learning approach was used [55]. RF has a long history in ecological studies and is shown to have a high classification accuracy when used in species distribution modelling [56]. Multicollinearity is common among remotely sensed variables and derived indices [18,57] and can lead to uncertainty within a model [58]. Multicollinearity between the predictor variables was addressed by calculating the variable inflation factors (VIFs) and the maximum linear correlation of each variable using the usdm package in R (version 4.2.2) [59]. Variables with high correlation (VIF > 0.8) were removed from consideration, resulting in 22 variables considered for model testing [18,60,61].

The selected model with optimal out-of-bag error and class error was then used to predict the probability of AWC occurrence throughout the study area. We converted the continuous prediction to a binary presence/absence map using the threshold where the sensitivity was equal to the specificity. The receiver-operator characteristic curve was calculated, and the area under the curve (AUC) was used to assess model accuracy. Finally, the model was spatially constrained, a posteriori, to only include the zones delineated in the LULC dataset (based on the Anderson Classification System) that are consistent with the ecological characteristics of AWC.

3. Results

3.1. Spectral Signatures and Phenology

The spectral signatures of the selected vegetation types and zones showed that AWC had a similar signature to that of other coniferous species within the study area (Figure 3). The deciduous and coniferous species exhibited clear differences during the leaf-on period in the red edge 2 and 3 (bands 6 and 7), and the NIR, and the NIR narrow regions (bands 8–8a). In the short-wave infrared bands (bands 11 and 12), there is little separation during the leaf-on period. During the leaf-off period, there is greater separation between the vegetation types in the short-wave infrared region. The spectral signatures of AWC and pitch pine (*Pinus rigida*) are extremely similar. However, there is subtle separation between these two species in the red edge, NIR, and NIR narrow regions during the leaf-on period (Figure 3), confirming that phenology considerations are important when considering remotely sensed data.

3.2. Species Distribution Model Evaluation

Atlantic White Cedar presence was best predicted by a combination of spectral and topographic variables selected during the model fitting process. The RF model used to predict AWC presence had an out-of-bag error of 7.2% and a maximized occurrence threshold of 0.32. The probability of AWC class presence and absence error was 11.9% and 4.4%, respectively, and the model predicted AWC with high accuracy, as indicated by an AUC value of 0.97. There were 11 variables included in the final model, and NDVI during the leaf-off period was the most important variable for predicting Atlantic White Cedar presence (Figure 4). Distance to water was the third most important variable in the model predictions, accounting for AWC preference to grow near streams and tidal areas. The NIR band (band 8) for both the leaf-on and leaf-off periods was retained in the model and potentially important to discriminate between AWC and pitch pine (Figure 3). The leaf-off VH band, a proxy for vegetation structure retained in the final model, was likely important in delineating AWC from deciduous and potentially other coniferous species with a different growth form.

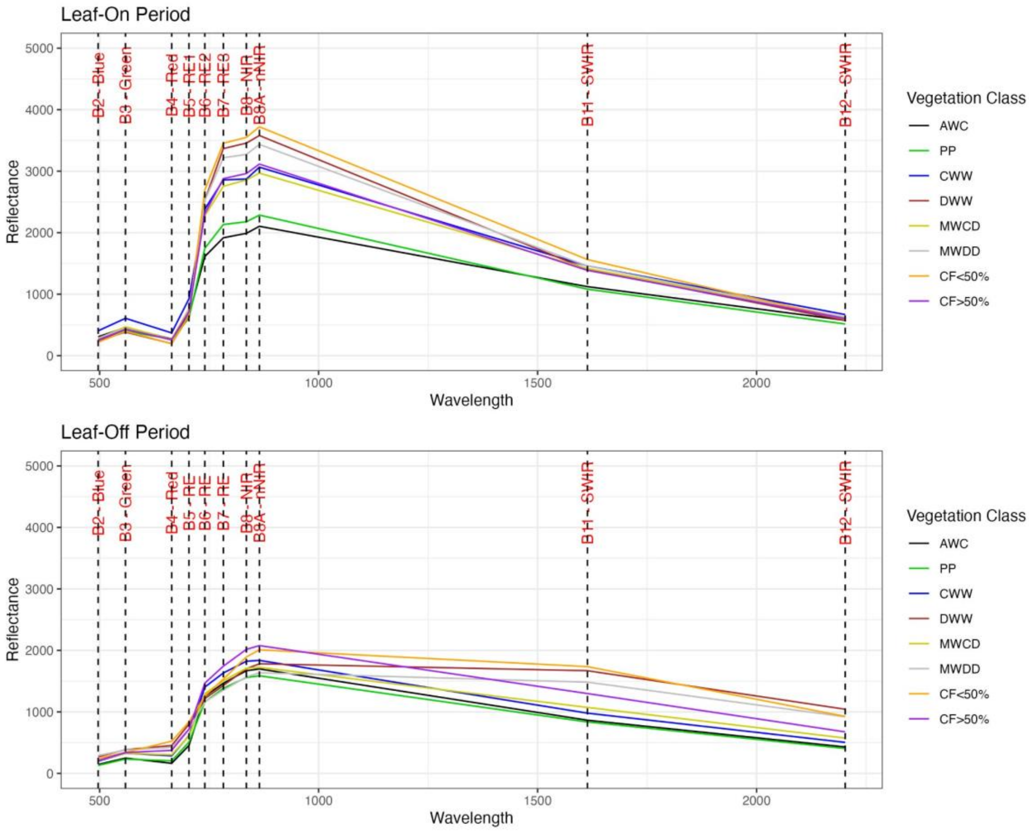

Figure 3. Spectral signatures of chosen classes to compare to AWC during the leaf-on period (top panel) and leaf-off period (bottom panel). AWC = Atlantic White Cedar, PP = Pitch Pine, CWW = Coniferous Wooded Wetland, CF < 50% = Coniferous Forest (10–50% crown closure), CF > 50% = Coniferous Forest (>50% crown closure), MWCD = Mixed Wooded Wetlands Coniferous Dominated, DWW = Deciduous Wooded Wetlands, MWDD = Mixed Wooded Wetlands Deciduous Dominated.

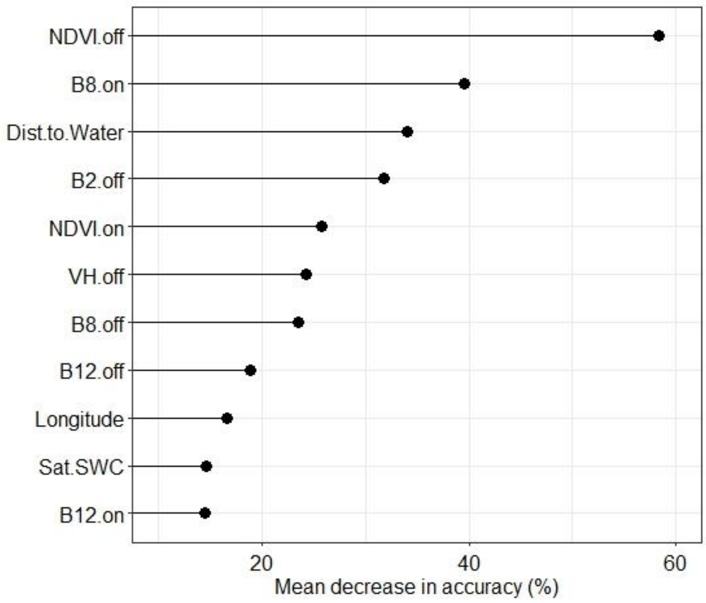

Figure 4. Variable importance plot for predictor variables used in the classification model. Higher values in mean decrease in accuracy on the x-axis indicate more important variables in the classification. Note: see Table 1 for predictor variable names; on refers to leaf-on periods, and off refers to leaf-off periods.

3.3. Atlantic White Cedar Mapping

The model output was used to create a spatially explicit map of AWC presence (Figure 5). The model was then spatially constricted to wetland zones and predicted 149 km^2 of AWC within those zones. The Atlantic White Cedar Wetlands class from the LULC map had the highest amount of the total predicted AWC (42.6%), followed by coniferous forest with greater than 50% crown closure (25.7%). The mean probability of occurrence mirrored the area of predicted AWC for each zone (Table 2). The predicted AWC showed strong agreement with aerial photographs at the stand scale (Figures 6 and 7). At the watershed scale (HUC-10), the vast majority of the predicted AWC occurs in the Wading River (39.4%) and Mullica River (33.8%) watersheds, which contain the majority of the protected areas in a number of state forests (Table 3).

Table 2. The percentage of total predicted AWC within the spatially constrained area of RF predictions by zone.

Zone Type	Percentage	Mean Probability
AWC Wetlands	42.6%	0.67
Coniferous Forest (>50% crown closure)	25.7%	0.46
Coniferous Wooded Wetlands	18.2%	0.5
Mixed Wooded Wetlands (Coniferous Dom.)	5.9%	0.48
Coniferous Forest (10–50% crown closure)	4.8%	0.44
Mixed Wooded Wetlands (Deciduous Dom.)	1.8%	0.46
Deciduous Wooded Wetlands	1.0%	0.43

Table 3. Amount of predicted AWC within each HUC-10 watershed. Percentages are the amount of the total predicted AWC within each watershed.

Name	Amount of Predicted AWC in Each Watershed (km^2)
Wading River	58.8 (39.4%)
Mullica River	50.4 (33.8%)
Lower Great Egg Harbor River	7.4 (5.0%)
Dennis Creek-Delaware Bay	7.1 (4.8%)
Manahawkin Bay-Little Egg Harbor	6.2 (4.2%)
Upper Great Egg Harbor River	6.0 (4.0%)
Lower Maurice River	5.2 (3.5%)
Barnegat Bay	4.8 (3.2%)
Tuckahoe River	1.8 (1.2%)
Great Egg Harbor Bay-Barrier Islands	1.3 (0.9%)

While the model was able to distinguish live AWC stands, it likely overpredicted in some of the upland areas, where pitch pine was more abundant. The model predicted 149 km^2 across the study area in the spatially constrained zones compared with the NJDEP 2012 dataset which identified 116 km^2 of AWC. Although the model may have overpredicted, the mapping effort could have missed AWC stands that were less conspicuous to aerial photography interpreters. However, the model only identifies 64 km^2 of live AWC inside the 2012 mapped AWC polygons, indicating a decrease of 51 km^2 (44%) of AWC between 2012 and 2021.

AWC mortality was documented both in the field and in aerial photographs throughout the study area. The model performed well to identify live AWC and distinguish it from dead AWC (Figures 8 and 9). The model did not predict live AWC in areas at the edge of the forest–marsh ecotone that were mapped as AWC prior to Hurricane Sandy (Figure 8). Aerial photo interpretation identified these areas as dead stands of AWC. Low-lying areas between the Bass and Wading Rivers experienced heavy flooding in the weeks after Hurricane Sandy and experienced large amounts of mortality confirmed in the field. The model was able to distinguish between the live and dead AWC (ghost forest) and correctly mapped the healthy, live stands (Figures 8 and 9).

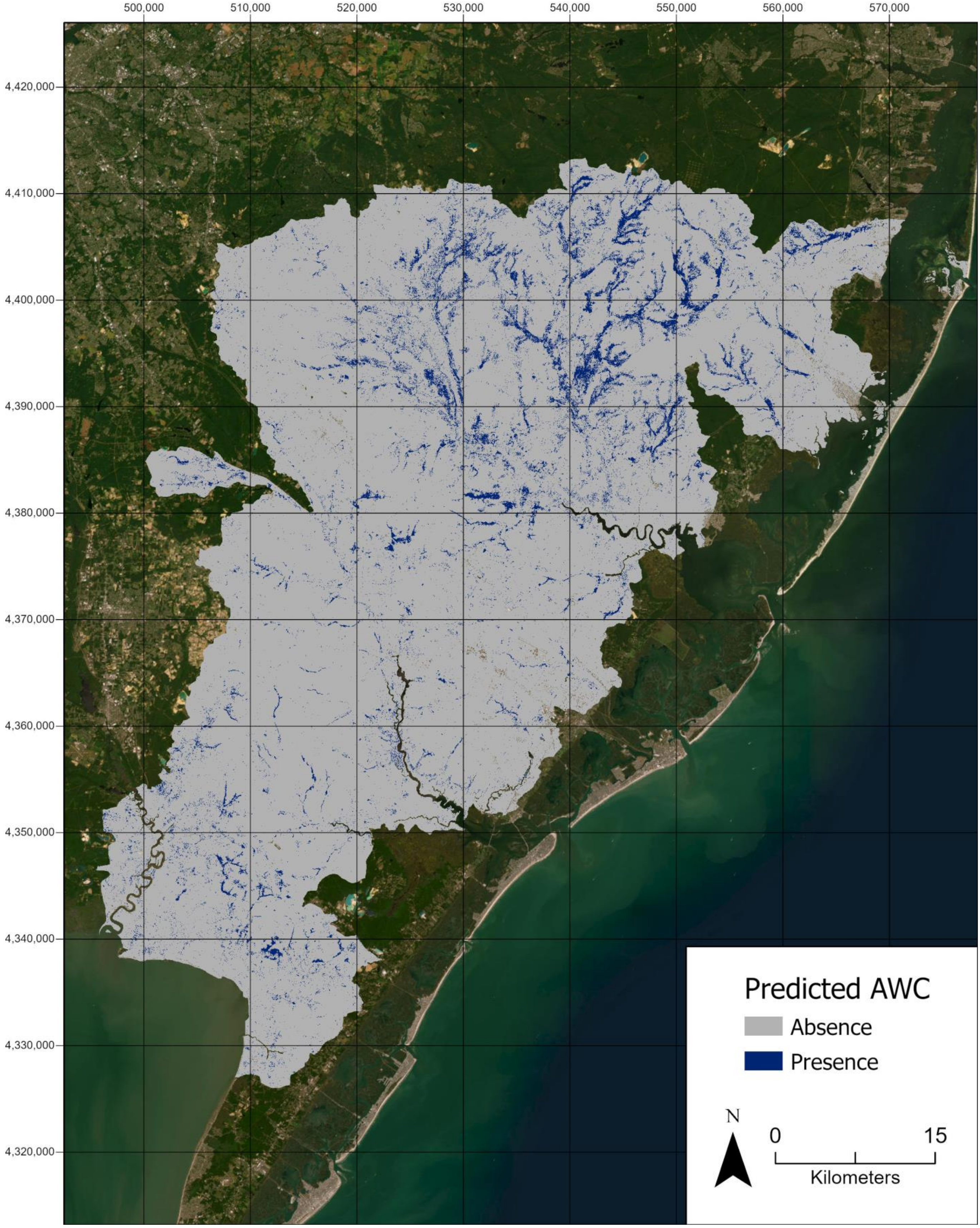

Figure 5. Spatially explicit prediction of AWC developed from the random forest model. The data are classified into AWC presence and absence based on a probability threshold of 0.32.

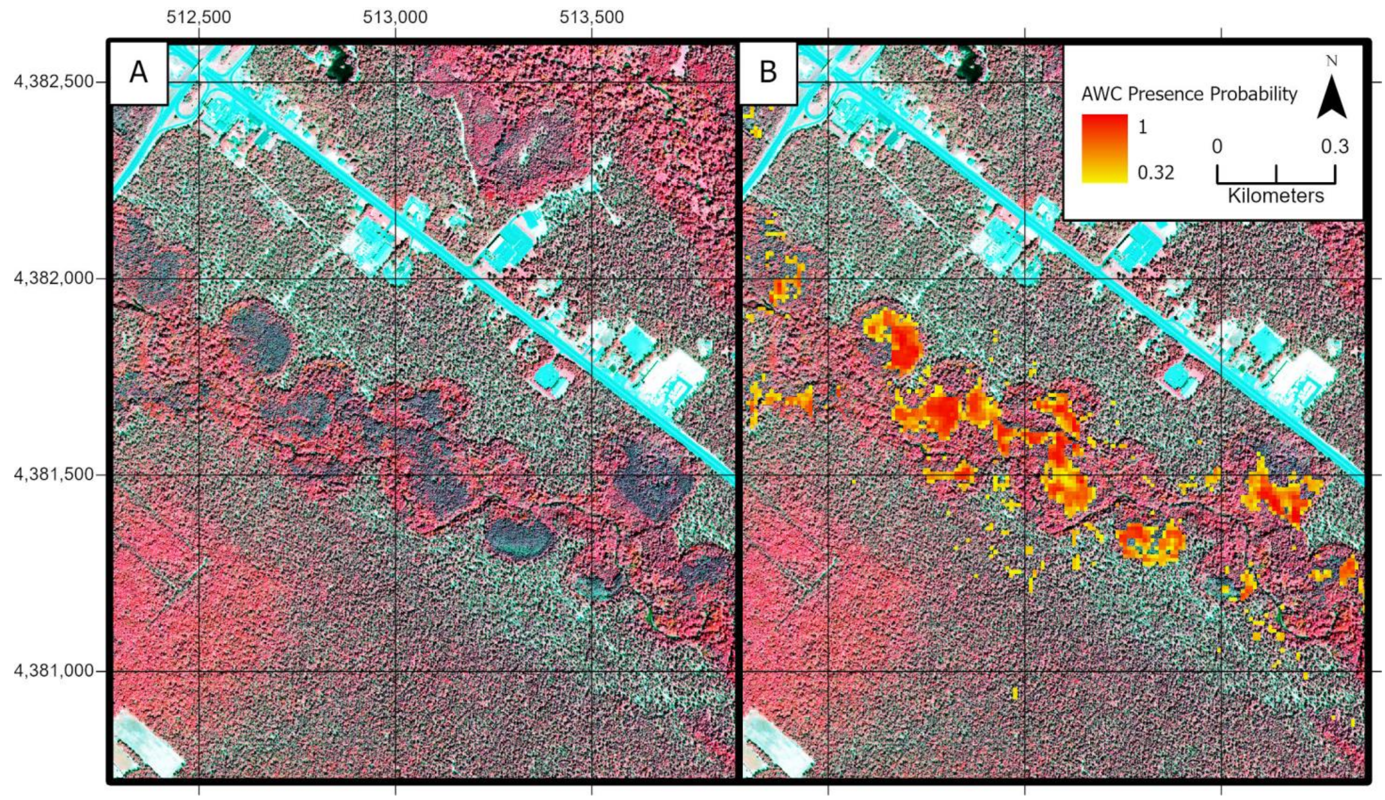

Figure 6. Panel (**A**)—AWC visible as areas of dark gray in NAIP color infrared imagery. Panel (**B**)—Model output of predicted probability of AWC presence. The model does not predict in adjacent areas of deciduous vegetation (appears red in color infrared).

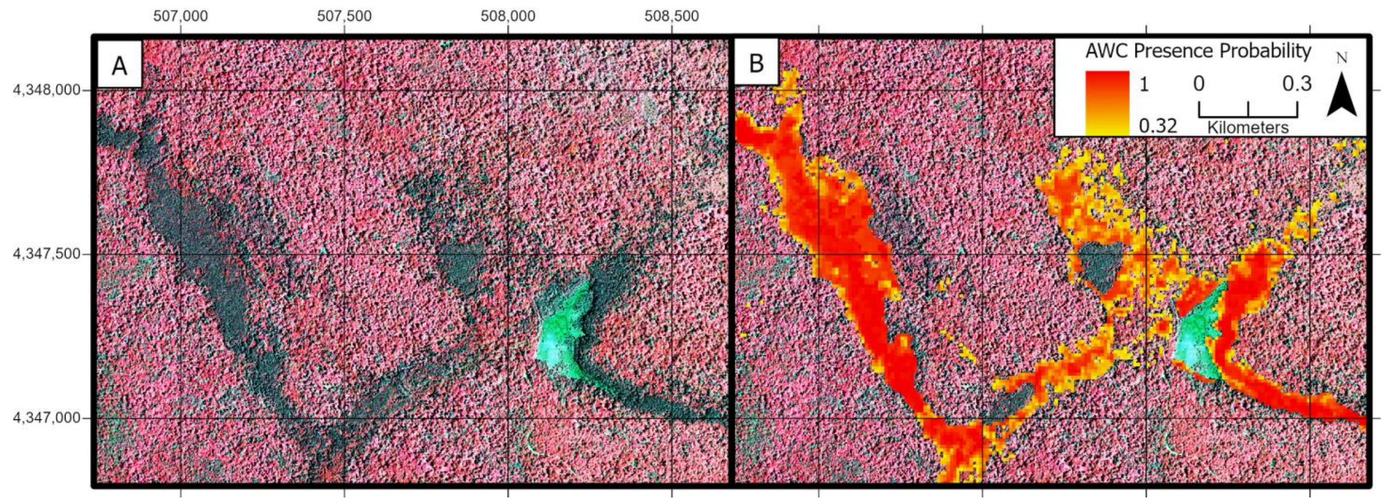

Figure 7. Panel (**A**)—Color infrared NAIP imagery of an area with AWC presence. Panel (**B**)—Model output of AWC presence closely follows the narrow bands of AWC on the landscape.

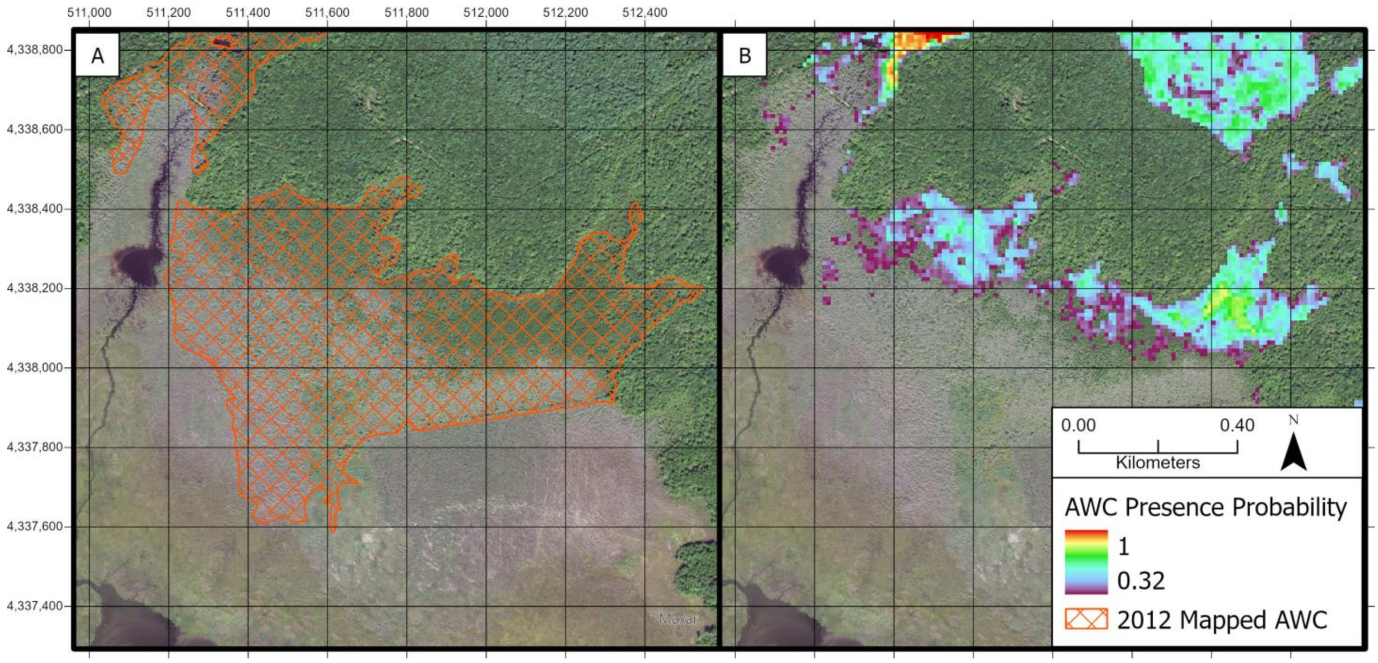

Figure 8. Panel (**A**)—Mapped AWC polygons from NJDEP (vintage 2012) overlaid on 2019 NAIP imagery. Areas of dead AWC are visible as large gray patches on the landscape inside the polygons. Panel (**B**)—The model only predicts where live patches of AWC exist and does not predict in locations of dead AWC stands.

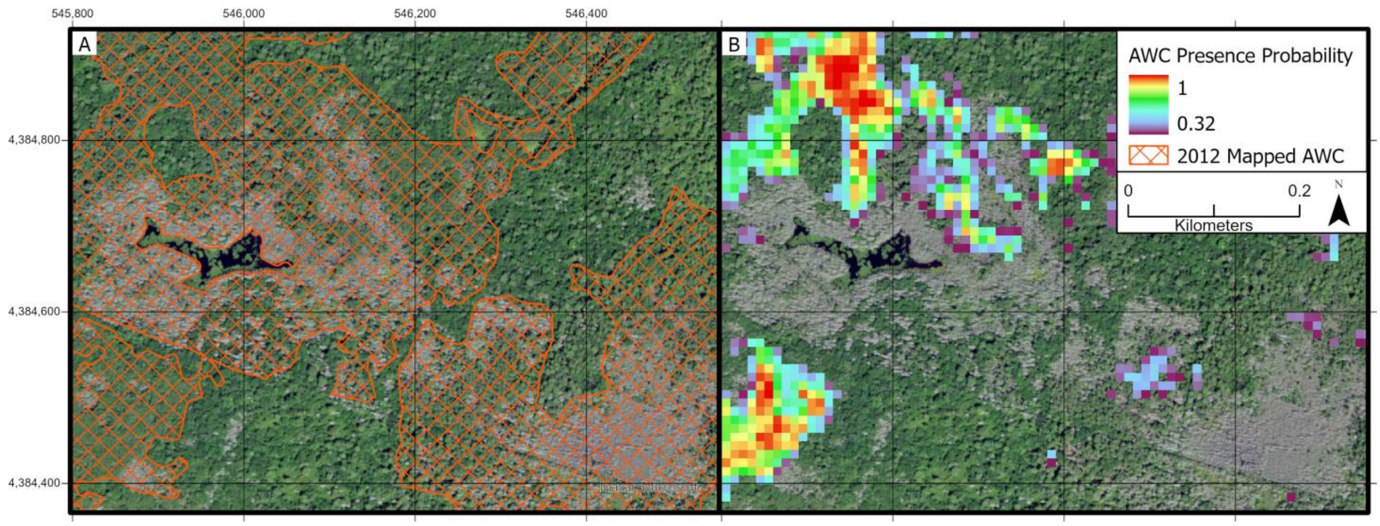

Figure 9. Panel (**A**)—Mapped AWC polygons from NJDEP (vintage 2012) overlaid on 2019 NAIP imagery. Areas of dead AWC are visible as large gray patches on the landscape that was confirmed with a field visit in 2022. Panel (**B**)—The model only predicts where live patches of AWC exist and does not predict AWC presence in the distinct areas of mortality.

4. Discussion

This model fills a needed data gap on the interaction of landscape position, soils, and hydrology on Atlantic White Cedar occurrence [62] and the driving variables of AWC presence in this region. Using an SDM is an improvement upon more traditional species distribution data types such as polygons or occurrence points because it uses fewer data to create distribution estimations, relies on open-source data, can be recreated for future time periods, and balances omission and commission errors, which are typically higher in distributions that are based solely on species occurrences or range maps [63]. The

2012 dataset, while useful and providing a good reference for this project, was created by updating a previous dataset using aerial photograph interpretation. It was limited by the minimum mapping unit and human interpretation. Furthermore, a severe disturbance event (Hurricane Sandy) occurred after that product was created, resulting in unmapped mortality of AWC. The RF model created here provides a transferable framework for the mapping of AWC throughout its range and is an improvement on previously created distribution maps.

4.1. Remote Sensing Is Critical in Mapping Atlantic White Cedar

It is not uncommon to have under- or overprediction within SDMs, which can either make the distribution of a species appear to be smaller or larger than it truly is. While SDMs may not always capture the true distribution of a species, they can be used as a hypothesis of where a species is located and how the species fares in different locations [64]. Although we were unable to include species interactions or dispersal constraints in our SDM [63,64], we were successful in identifying the current distribution of live, healthy AWC stands (Figure 5). Furthermore, the model can be utilized as a tool for tracking changes in the distribution of this species across the landscape. The model was developed using fine-scale (~10 m) data, which enabled small stands of AWC to be mapped across this landscape. The framework relies on open-source data and is, therefore, transferrable to model other areas within AWC's range. Consideration of a large suite of potential predictor variables allowed the modelling process to identify those most important for predicting AWC presence (Figure 4). Eight of the eleven predictor variables were from satellite data, highlighting the value of including remotely sensed data and phenology insight into species distribution models.

Our results show that there has been a loss of AWC in some areas that were previously mapped as live AWC, as the model is able to distinguish between the live and dead AWC (Figures 8 and 9). We identified a 44% loss of AWC between 2012 and 2021 in southern New Jersey. There is clear aerial photographic evidence that some of this stand loss occurred since 2012. However, a qualitative assessment of aerial photos from the 2000s identified small pockets of mortality within 2012 mapped stands, suggesting that the AWC dataset had not been updated during that period, thus making direct comparisons difficult. Moving forward, this model could be used to quantify and track AWC loss across a landscape due to climate change or other pressures in the future. Sea-level rises, inundation, and more frequent and intense storms all present a threat to AWC, as this species is sensitive to changes in the water level and salinity. These issues are especially pressing in the Mid-Atlantic region, which has the highest rates of SLR globally [9] and will continue to press AWC further inland in areas where the migration is not blocked by urbanization. The conversion of AWC to ghost forest has been documented by other researchers as well [4,7]. In this study we extend that knowledge and document AWC conversion to ghost forest in a new region. Furthermore, the model presented here can be extended to future time periods to track those changes across the landscape and determine which stands are experiencing increased stress or mortality.

4.2. Ecological and Technological Considerations

The model had a low error component with reasonable predictions of AWC presence; however, there were some areas of overprediction (Figure 8). Overprediction within an SDM occurs when the model predicts the species to have a broader distribution than reality due to the inadequate capture of biotic interactions or dispersal constraints on the species [63]. We believe there are a few reasons for overprediction in the model. First, the available data might be too coarse to capture fine scale variability across the landscape. SDMs should be created at a scale relevant to biological interactions, and for many sessile species (such as plants), it is necessary to use smaller scales to produce models with high predictive capabilities [65]. For all the datasets to match in resolution, we chose to use more coarse-scale abiotic variables (10 m) than were available to match the scale of the spectral variables. Using finer-scale abiotic variables would have required scaling up datasets, which can cause issues with fine-scale heterogeneity, interactions, nonlinearity, and feedbacks [66]. To maintain the integrity of the data, coarser-scale abiotic variables were used to best match the resolution of the Sentinel-1 and Sentinel-2A bands. The coarser spatial scale of the datasets likely contributed to the overprediction in the model due to the generalization of the underlying environmental conditions. Mapping narrow, linear vegetation patterns on the landscape similar to AWC presents a challenge with satellite data [18]. Furthermore, AWC is influenced by changes in microtopography [14], and the spatial resolution of 10 m may not have been adequate to detect those fine-scale changes in topography.

While RF models are known for their utility within ecology and their high classification accuracy within SDMs, there are some limitations when creating an SDM utilizing a machine learning approach, such as overfitting in some cases [24]. Random forests provide more accurate predictions across a landscape than other methods, but if RF is used to extrapolate and project those predictions to an area outside of the placement of the training data provided, there can be some resulting issues with both over- and underprediction [67].

Another potential reason for the overprediction in the model may have been the placement of the presence and absence points used in the training data (Figure 1). There may have been AWC in locations that were not truly suitable for species to live long term, such as in relict populations, and there may have been absence points placed in areas that are truly suitable for this species, but no AWC was present due to dispersal limitations, biotic interactions, or environmental stochasticity [64]. It is advised to avoid placing absence points in an area near presence points [68]. However, the small study area made the placement of points an appropriate distance apart from each other more challenging. The placement of the presence and absence points may not have represented the true niche of this species, and the distance between the presence and absence points may not have been large enough to provide the necessary variability in the data to help the model distinguish between AWC and the other nearby classes.

Overprediction in SDMs is a common issue, and many studies do not find clear support for their model predictions [64]. In this study, we attempted to correct for the overprediction by adding variables that we had not previously considered, as well as spatially constraining the model to only predict within areas that are ecologically relevant to the study. The most frequent model overprediction correction approach is the use of geographical barriers [63], which was performed here by determining ecologically appropriate spatial zones, then constraining the model predictions to those areas. Spatially constraining the model allowed us to identify and remove predictions from the model output that fell within zones that clearly did not contain AWC and those where it was unlikely that AWC was present. It can be challenging to identify if an area is truly overpredicted without quantitative field data; our assumptions of overpredicted areas are based on our interpretation of the aerial imagery and known AWC locations. Even in light of these considerations, the SDM presented here correctly identified live pixels of AWC in a matrix of live and dead AWC (Figure 8), as well as distinguished AWC pixels from the surrounding deciduous vegetation (Figure 6).

There are a number of other coniferous species present, such as pitch pine, which is the most common pine throughout the New Jersey Pinelands. Pitch pine can be codominant within AWC stands in New Jersey [25] and has a very similar spectral response to AWC (Figure 3), which could potentially be contributing to the overprediction in the model. The spectral response of a given pixel is an amalgamation of all elements, including other conifer species, present in the pixel [69,70]. Spectral variables were important predictors in the SDM (Figure 4); therefore, if multiple species had similar responses, it is likely that this would cause the model to predict those areas as AWC, especially if it was a species that can exist in the same underlying environmental conditions, such as pitch pine. We believe it is advantageous to document the spectral response of AWC using the expanded spectral capabilities of Sentinel-2A. Advances in future sensors will likely provide more spectral information that could be used to build upon the work presented here.

4.3. Management Implications for Atlantic White Cedar

Atlantic White Cedar is facing increasing mortality along the coast in the face of anthropogenic climate change. Species within the marsh–forest ecotone will respond differently to these environmental changes [2], and the ghost forests provide the opportunity to track the migration of species within the marsh–forest ecotone. The marsh–forest ecotone is shifting in response to increasing storms and sea-level rises [3], and AWC is one of the most conspicuous species that is experiencing loss from these disturbances. After Hurricane Sandy in 2012, there were notable AWC ghost forests in southern New Jersey [5], and many of these areas did not recover post-hurricane. The model was able to distinguish between live and dead AWC (Figures 8 and 9), which allows for the tracking of AWC loss at the stand level to be monitored over time. Knowledge of where some potential areas for active management (e.g., planting new trees) or maintaining the live, healthy stands is important to have to help best protect and preserve this species in this region.

We created a transferable model that documents the baseline amount of Atlantic White Cedar throughout southern New Jersey. The use of random forests in species distribution models is beneficial for inventory and monitoring purposes as these models are run without a priori assumptions about the ecological influences of variables on the species, allowing them to better predict a species across space than some traditional SDM methods [71]. In areas where there is limited information about underlying processes, species interactions, dispersal limits, and nonlinear relationships, the use of RF models can help create a model with the best predictive capabilities without knowing any of the information about which processes may be influencing a species distribution across a landscape. The information provided from SDMs can be used to monitor species and help create management and loss mitigation strategies to conserve species in the future. In coastal regions, it is very challenging to predict where and when storm surges will occur [72]; however, SDMs provide information that could help managers locate stands of trees that may be in an area that is more susceptible to these threats. The model outputs capture the loss of AWC on the landscape in recent years, as the model was able to distinguish areas of mortality (Figures 8 and 9). This work provides much needed information to managers about AWC stands and helps us better understand stand dynamics (Table 3). Illuminating which environmental drivers were the most important to AWC within the model provides insight into what drives the distribution of the species across the landscape. Distance to water was the third most important predictor of AWC presence (Figure 4), which was not surprising given this species thrives only within 200 km of the coast [14] and tends to grow along streams and rivers [15] (Figure 6). These areas are more susceptible to inundation from sea-level rises or storm surges and may be more at risk of experiencing loss of AWC and stands within these areas should be carefully monitored.

Our analysis demonstrates that Atlantic White Cedar stands are dynamic and have experienced change since Hurricane Sandy (2012). The use of predictive habitat distribution modelling, using both remotely sensed and abiotic variables, is an effective method for the mapping of species distributions for use in management and loss mitigation. This work demonstrates the importance of including remotely sensed variables in species distribution models [27] (Figure 4). The use of SDMs to create spatially explicit maps of species distributions that are difficult to map using field methods is an important data gap to address due to the pressures of climate change on this important ecotone.

5. Conclusions

In this study, we aimed to create a spatially explicit map of Atlantic White Cedar presence throughout southern New Jersey. To help meet this goal, we determined the driving variables of AWC presence as well as the spectral signature of AWC compared to surrounding vegetation types to better understand the dynamics of this important, sensitive species. A combination of field methods and aerial photograph interpretation allowed for the creation of a training dataset that was used to create a random forests model. The results showed that both remotely sensed and abiotic variables were important in predicting AWC presence and that there has been some AWC mortality experienced on the landscape. The model presented in this study provides high utility for AWC management and tracking mortality dynamics within stands after disturbances such as hurricanes. This study established a baseline on the amount and locations of AWC occurrence throughout southern New Jersey. Our work can be extended across the full distribution of the species and applied to future time periods to track those changes across the landscape to assess changing environmental conditions. Additional research can build on the work presented here by utilizing new sensors, such as those mounted on unmanned aerial vehicles. These would provide imagery with finer resolution and incorporate additional field data to understand if and why overprediction occurs in the model.

Author Contributions: Conceptualization, B.N. and T.J.A.; methodology, B.N., A.E.S., A.L.C. and T.J.A.; formal analysis, B.N. and T.J.A.; data curation, B.N.; writing—original draft preparation, B.N. and T.J.A.; writing—review and editing, B.N., A.E.S., A.L.C. and T.J.A.; visualization, B.N. and T.J.A.; supervision, T.J.A. All authors have read and agreed to the published version of the manuscript.

Funding: This research received no external funding.

Data Availability Statement: All satellite data used in this study are publicly available through Google Earth Engine. Field-collected data and unique abiotic variables (e.g., distance to water) created for this research have been archived in the Knowledge Network for Biocomplexity [73]. R code for analysis is available from the corresponding author upon request.

Acknowledgments: We thank Stephanie Burkey and Kathryn Burns for field assistance. We gratefully acknowledge financial support from the Department of Geography at Kent State University.

Conflicts of Interest: The authors declare no conflicts of interest.

References

1. Schieder, N.W.; Kirwan, M.L. Sea-Level Driven Acceleration in Coastal Forest Retreat. *Geology* **2019**, *47*, 1151–1155. [CrossRef]
2. Jobe, J.G.D.; Gedan, K. Species-Specific Responses of a Marsh-Forest Ecotone Plant Community Responding to Climate Change. *Ecology* **2021**, *102*, e03296. [CrossRef]
3. Fagherazzi, S.; Nordio, G.; Munz, K.; Catucci, D.; Kearney, W.S. Variations in Persistence and Regenerative Zones in Coastal Forests Triggered by Sea Level Rise and Storms. *Remote Sens.* **2019**, *11*, 2019. [CrossRef]
4. Able, K.W. Special Issue: Concepts and Controversies in Tidal Marsh Ecology Revisited From Cedar Cemeteries to Marsh Lakes: A Case Study of Sea-Level Rise and Habitat Change in a Northeastern US Salt Marsh. *Estuaries Coasts* **2021**, *44*, 1649–1657. [CrossRef]
5. Doyle, J.M.; Earley, K.E.; Atkinson, R.B. An Analysis of Atlantic White Cedar (*Chaemaecyparis thyoides* (L.) B.S.P.) Tree Rings as Indicators of Ghost Forest Development in a Globally Threatened Ecosystem. *Forests* **2021**, *12*, 973. [CrossRef]
6. Hauser, S.; Meixler, M.S.; Laba, M. Quantification of Impacts and Ecosystem Services Loss in New Jersey Coastal Wetlands Due to Hurricane Sandy Storm Surge. *Wetlands* **2015**, *35*, 1137–1148. [CrossRef]
7. Ury, E.A.; Yang, X.; Wright, J.P.; Bernhardt, E.S. Rapid Deforestation of a Coastal Landscape Driven by Sea-Level Rise and Extreme Events. *Ecol. Appl.* **2021**, *31*, e02339. [CrossRef]
8. Woods, N.N.; Swall, J.L.; Zinnert, J.C. Soil Salinity Impacts Future Community Composition of Coastal Forests. *Wetlands* **2020**, *40*, 1495–1503. [CrossRef]
9. Kopp, R.E.; Andrews, C.; Broccoli, A.; Garner, A.; Kreeger, D.; Leichenko, R.; Lin, N.; Little, C.; Miller, J.A.; Miller, J.K.; et al. *New Jersey's Rising Seas and Changing Coastal Storms: Report of the 2019 Science and Technical Advisory Panel*; The State University of New Jersey: New Brunswick, NJ, USA, 2019.
10. Cooper, M.J.P.; Beevers, M.D.; Oppenheimer, M. The Potential Impacts of Sea Level Rise on the Coastal Region of New Jersey, USA. *Clim. Chang.* **2008**, *90*, 475–492. [CrossRef]
11. Smith, A.J.; Goetz, E.M. Climate Change Drives Increased Directional Movement of Landscape Ecotones. *Landsc. Ecol.* **2021**, *36*, 3105–3116. [CrossRef]
12. Hasse, J.E.; Lathrop, R.G.; Bognar, J.A. *Changing Landscapes in the Garden State: Land Use Change in NJ 1986 Thru 2012*; Rutgers University: New Brunswick, NJ, USA; Rowan University: Glassboro, NJ, USA, 2016.
13. The American Littoral Society; National Fish and Wildlife Foundation. Assessing the Impacts of Hurricane Sandy. 2012. Available online: https://rucore.libraries.rutgers.edu/rutgers-lib/43631/ (accessed on 19 September 2024).
14. Hnatkovich, A.M.; Yorks, T.E. Current Status and Future Development of the Only *Chamaecyparis thyoides* (Atlantic White-Cedar) Population in Pennsylvania. *Nat. Areas J.* **2009**, *29*, 216–223. [CrossRef]

15. Little, S.J. Ecology and Silviculture of Whitecedar and Associated Hardwoods in Southern New Jersey. *Yale Sch. For. Environ. Stud. Bull. Ser.* **1950**, *54*, 134.
16. Crawford, E.R.; Day, F.P.; Atkinson, R.B. Influence of Environment and Substrate Quality on Root Decomposition in Naturally Regenerating and Restored Atlantic White Cedar Wetlands. *Wetlands* **2007**, *27*, 1–11. [CrossRef]
17. Laing, J.M.; Shear, T.H.; Blazich, F.A. How Management Strategies Have Affected Atlantic White-Cedar Forest Recovery after Massive Wind Damage in the Great Dismal Swamp. *For. Ecol. Manag.* **2011**, *262*, 1337–1344. [CrossRef]
18. Assal, T.J.; Steen, V.A.; Caltrider, T.; Cundy, T.; Stewart, C.; Manning, N.; Anderson, P.J. Monitoring Long-Term Riparian Vegetation Trends to Inform Local Habitat Management in a Mountainous Environment. *Ecol. Indic.* **2021**, *127*, 107807. [CrossRef]
19. Assal, T.J.; Anderson, P.J.; Sibold, J. Mapping Forest Functional Type in a Forest- Shrubland Ecotone Using SPOT Imagery and Predictive Habitat Distribution Modelling. *Remote Sens. Lett.* **2015**, *6*, 755–764. [CrossRef]
20. Hailu, B.T.; Siljander, M.; Maeda, E.E.; Pellikka, P. Assessing Spatial Distribution of *Coffea arabica* L. in Ethiopia's Highlands Using Species Distribution Models and Geospatial Analysis Methods. *Ecol. Inform.* **2017**, *42*, 79–89. [CrossRef]
21. He, Y.; Chen, G.; Potter, C.; Meentemeyer, R.K. Integrating Multi-Sensor Remote Sensing and Species Distribution Modeling to Map the Spread of Emerging Forest Disease and Tree Mortality. *Remote Sens. Environ.* **2019**, *231*, 111238. [CrossRef]
22. Smith, A.B.; Murphy, S.J.; Henderson, D.; Erickson, K.D. Including Imprecisely Georeferenced Specimens Improves Accuracy of Species Distribution Models and Estimates of Niche Breadth. *Glob. Ecol. Biogeogr.* **2023**, *32*, 342–355. [CrossRef]
23. Elith, J.; Leathwick, J.R. Species Distribution Models: Ecological Explanation and Prediction across Space and Time. *Annu. Rev. Ecol. Evol. Syst.* **2009**, *40*, 677–697. [CrossRef]
24. Pecchi, M.; Marchi, M.; Burton, V.; Giannetti, F.; Moriondo, M.; Bernetti, I.; Bindi, M.; Chirici, G. Species Distribution Modelling to Support Forest Management. A Literature Review. *Ecol. Model.* **2019**, *411*, 108817. [CrossRef]
25. Laderman, A.D. *The Ecology of Atlantic White Cedar Wetlands: A Community Profile*; U.S. Department of Interior, Fish and Wildlife Service, National Wetlands Research Center: Washington, DC, USA, 1989.
26. Zimmermann, N.E.; Edwards, T.C.J.; Moisen, G.G.; Frescino, T.S.; Blackard, J.A. Remote Sensing-Based Predictors Improve Distribution Models of Rare, Early Successional and Broadleaf Tree Species in Utah. *J. Appl. Ecol.* **2007**, *44*, 1057–1067. [CrossRef]
27. Cord, A.; Rödder, D. Inclusion of Habitat Availability in Species Distribution Models through Multi-Temporal Remote-Sensing Data? *Ecol. Appl.* **2011**, *21*, 3285–3298. [CrossRef]
28. Jones, H.G.; Vaughan, R.H. *Remote Sensing of Vegetation: Principles, Techniques, and Applications*; OUP Oxford: Oxford, UK, 2010.
29. Price, J.C. How Unique Are Spectral Signatures? *Remote Sens. Environ.* **1994**, *49*, 181–186. [CrossRef]
30. Rajakumari, S.; Mahesh, R.; Sarunjith, K.J.; Ramesh, R. Building Spectral Catalogue for Salt Marsh Vegetation, Hyperspectral and Multispectral Remote Sensing. *Reg. Stud. Mar. Sci.* **2022**, *53*, 102435. [CrossRef]
31. Estrada, F.; Flexas, J.; Araus, J.L.; Mora-Poblete, F.; Gonzalez-Talice, J.; Castillo, D.; Matus, I.A.; Méndez-Espinoza, A.M.; Garriga, M.; Araya-Riquelme, C.; et al. Exploring Plant Responses to Abiotic Stress by Contrasting Spectral Signature Changes. *Front. Plant Sci.* **2023**, *13*, 1026323. [CrossRef]
32. Bhattarai, R.; Rahimzadeh-Bajgiran, P.; Weiskittel, A.; Meneghini, A.; MacLean, D.A. Spruce Budworm Tree Host Species Distribution and Abundance Mapping Using Multi-Temporal Sentinel-1 and Sentinel-2 Satellite Imagery. *ISPRS J. Photogramm. Remote Sens.* **2021**, *172*, 28–40. [CrossRef]
33. Akbari, V.; Solberg, S.; Puliti, S. Multitemporal Sentinel-1 and Sentinel-2 Images for Characterization and Discrimination of Young Forest Stands under Regeneration in Norway. *IEEE J. Sel. Top. Appl. Earth Obs. Remote Sens.* **2021**, *14*, 5049–5063. [CrossRef]
34. United States Geological Survey, U.S.G.S. National Hydrography Dataset Plus High Resolution. Available online: https://www.sciencebase.gov/catalog/item/5d30c268e4b01d82ce84a923 (accessed on 9 September 2022).
35. Bunnell, J.F.; Zampella, R.A.; Lathrop, R.G.; Bognar, J.A. Landscape Changes in the Mullica River Basin of the Pinelands National Reserve, New Jersey, USA. *Environ. Manag.* **2003**, *31*, 696–708. [CrossRef]
36. Miao, Z.; Lathrop, R.G.; Xu, M.; La Puma, I.P.; Clark, K.L.; Hom, J.; Skowronski, N.; Van Tuyl, S. Simulation and Sensitivity Analysis of Carbon Storage and Fluxes in the New Jersey Pinelands. *Environ. Model. Softw.* **2011**, *26*, 1112–1122. [CrossRef]
37. Zampella, R.A.; Lathrop, R.G. Landscape Changes in Atlantic White Cedar (*Chamaecyparis thyoides*) Wetlands of the New Jersey Pinelands. *Landsc. Ecol.* **1997**, *12*, 397–408. [CrossRef]
38. United States Department of Agriculture. Ortho NAIP. Available online: https://nrcs.app.box.com/v/naip/folder/95484293573 (accessed on 21 February 2022).
39. NJDEP Bureau of GIS. Land Use/Land Cover of New Jersey 2012. Available online: https://www.nj.gov/dep/gis/digidownload/zips/OpenData/Land_lu_2012.zip (accessed on 25 February 2022).
40. Fernández-Guisuraga, J.M.; Suárez-Seoane, S.; Calvo, L. Radar and Multispectral Remote Sensing Data Accurately Estimate Vegetation Vertical Structure Diversity as a Fire Resilience Indicator. *Remote Sens. Ecol. Conserv.* **2023**, *9*, 117–132. [CrossRef]
41. Koley, S.; Chockalingam, J. Sentinel 1 and Sentinel 2 for Cropland Mapping with Special Emphasis on the Usability of Textural and Vegetation Indices. *Adv. Sp. Res.* **2022**, *69*, 1768–1785. [CrossRef]
42. R Core Team. *R: A Language and Environment for Statistical Computing 2022*; R Core Team: Vienna, Austria, 2022.
43. Hijmans, R.J. Raster: Geographic Data Analysis and Modeling. 2023. Available online: https://cran.r-project.org/web/packages/raster/raster.pdf (accessed on 19 September 2024).

44. Rouse, J.W.; Haas, R.H.; Schell, J.A.; Deering, D.W.; Harlan, J.C. *Monitoring the Vernal Advancements and Retrogradation of Natural Vegetation*; Final Report; NASA/GSFC: Greenbelt, MD, USA, 1974; pp. 1–137.
45. Sims, D.A.; Gamon, J.A. Relationships between Leaf Pigment Content and Spectral Reflectance across a Wide Range of Species, Leaf Structures and Developmental Stages. *Remote Sens. Environ.* **2002**, *81*, 337–354. [CrossRef]
46. De Reu, J.; Bourgeois, J.; Bats, M.; Zwertvaegher, A.; Gelorini, V.; De Smedt, P.; Chu, W.; Antrop, M.; De Maeyer, P.; Finke, P.; et al. Application of the Topographic Position Index to Heterogeneous Landscapes. *Geomorphology* **2013**, *186*, 39–49. [CrossRef]
47. Sørensen, R.; Zinko, U.; Seibert, J. On the Calculation of the Topographic Wetness Index: Evaluation of Different Methods Based on Field Observations. *Hydrol. Earth Syst. Sci.* **2006**, *10*, 101–112. [CrossRef]
48. Riley, S.J.; DeGloria, S.D.; Elliot, R. Terrain_Ruggedness_Index.Pdf. *Intermt. J. Sci.* **1999**, *5*, 23–27.
49. Ponti, R.; Sannolo, M. The Importance of Including Phenology When Modelling Species Ecological Niche. *Ecography* **2023**, *2023*, e06143. [CrossRef]
50. Roberts, D.A.; Ustin, S.L.; Ogunjemiyo, S.; Greenberg, J.; Bobrowski, S.Z.; Chen, J.; Hinckley, T.M. Spectral and Structural Measures of Northwest Forest Vegetation at Leaf to Landscape Scales. *Ecosystems* **2004**, *7*, 545–562. [CrossRef]
51. Williams, D.L. A Comparison of Spectral Reflectance Properties at the Needle, Branch, and Canopy Level for Selected Conifer Species. *Remote Sens. Environ.* **1991**, *35*, 79–93. [CrossRef]
52. NJDEP Bureau of GIS. Coastline (2012) of New Jersey. Available online: https://gisdata-njdep.opendata.arcgis.com/datasets/njdep::coastline-2012-of-new-jersey/about (accessed on 11 June 2022).
53. NJDEP Bureau of GIS. Head of Tide for New Jersey Watercourses. Available online: https://gisdata-njdep.opendata.arcgis.com/datasets/njdep::head-of-tide-hot-for-new-jersey-watercourses/about (accessed on 14 June 2022).
54. Chaney, N.W.; Minasny, B.; Herman, J.D.; Nauman, T.W.; Brungard, C.W.; Morgan, C.L.S.; McBratney, A.B.; Wood, E.F.; Yimam, Y. POLARIS Soil Properties: 30-m Probabilistic Maps of Soil Properties Over the Contiguous United States. *Water Resour. Res.* **2019**, *55*, 2916–2938. [CrossRef]
55. Liaw, A.; Wiener, M. Classification and Regression by RandomForest. *R J.* **2002**, *2*, 18–22.
56. Cutler, D.R.; Edwards, T.C.; Beard, K.H.; Cutler, A.; Hess, K.T.; Gibson, J.; Lawler, J.J. Random Forests for Classification in Ecology. *Ecology* **2007**, *88*, 2783–2792. [CrossRef] [PubMed]
57. Engler, R.; Waser, L.T.; Zimmermann, N.E.; Schaub, M.; Berdos, S.; Ginzler, C.; Psomas, A. Combining Ensemble Modeling and Remote Sensing for Mapping Individual Tree Species at High Spatial Resolution. *For. Ecol. Manag.* **2013**, *310*, 64–73. [CrossRef]
58. De Marco Junior, P.; Nóbrega, C.C. Evaluating Collinearity Effects on Species Distribution Models: An Approach Based on Virtual Species Simulation. *PLoS ONE* **2018**, *13*, 0202403. [CrossRef]
59. Naimi, B.; Hamm, N.A.S.; Groen, T.A.; Skidmore, A.K.; Toxopeus, A.G. Where Is Positional Uncertainty a Problem for Species Distribution Modelling. *Ecography* **2014**, *37*, 191–203. [CrossRef]
60. Jarnevich, C.S.; Esaias, W.E.; Ma, P.L.A.; Morisette, J.T.; Nickeson, J.E.; Stohlgren, T.J.; Holcombe, T.R.; Nightingale, J.M.; Wolfe, R.E.; Tan, B. Regional Distribution Models with Lack of Proximate Predictors: Africanized Honeybees Expanding North. *Divers. Distrib.* **2014**, *20*, 193–201. [CrossRef]
61. Werkowska, W.; Márquez, A.L.; Real, R.; Acevedo, P. A Practical Overview of Transferability in Species Distribution Modeling. *Environ. Rev.* **2017**, *25*, 127–133. [CrossRef]
62. Keeland, B.D.; McCoy, J.W. Plant Community Composition of a Tidally Influenced, Remnant Atlantic White Cedar Stand in Mississippi. In *Ecology of Tidal Freshwater Forested Wetlands of the Southeastern United States*; Springer: Berlin/Heidelberg, Germany, 2007; pp. 89–112, ISBN 9781402050947.
63. Velazco, S.J.E.; Ribeiro, B.R.; Laureto, L.M.O.; De Marco Júnior, P. Overprediction of Species Distribution Models in Conservation Planning: A Still Neglected Issue with Strong Effects. *Biol. Conserv.* **2020**, *252*, 108822. [CrossRef]
64. Lee-Yaw, J.A.; McCune, J.L.; Pironon, S.; Sheth, S.N. Species Distribution Models Rarely Predict the Biology of Real Populations. *Ecography* **2022**, *2022*, e05877. [CrossRef]
65. Chauvier, Y.; Descombes, P.; Guéguen, M.; Boulangeat, L.; Thuiller, W.; Zimmermann, N.E. Resolution in Species Distribution Models Shapes Spatial Patterns of Plant Multifaceted Diversity. *Ecography* **2022**, *2022*, e05973. [CrossRef]
66. Fritsch, M.; Lischke, H.; Meyer, K.M. Scaling Methods in Ecological Modelling. *Methods Ecol. Evol.* **2020**, *11*, 1368–1378. [CrossRef]
67. Heikkinen, R.K.; Marmion, M.; Luoto, M. Does the Interpolation Accuracy of Species Distribution Models Come at the Expense of Transferability? *Ecography* **2012**, *35*, 276–288. [CrossRef]
68. Lobo, J.M.; Jiménez-Valverde, A.; Hortal, J. The Uncertain Nature of Absences and Their Importance in Species Distribution Modelling. *Ecography* **2010**, *33*, 103–114. [CrossRef]
69. Assal, T.J.; Sibold, J.; Reich, R. Modeling a Historical Mountain Pine Beetle Outbreak Using Landsat MSS and Multiple Lines of Evidence. *Remote Sens. Environ.* **2014**, *155*, 275–288. [CrossRef]
70. Lefsky, M.A.; Cohen, W.B. Selection of Remotely Sensed Data. In *Remote Sensing of Forest Environments: Concepts and Case Studies*; Wulder, M.A., Franklin, S.E., Eds.; Springer: Boston, MA, USA, 2003; pp. 13–46, ISBN 1402074050.
71. Magness, D.R.; Huettmann, F.; Morton, J.M. Using Random Forests to Provide Predicted Species Distribution Maps as a Metric for Ecological Inventory & Monitoring Programs. *Stud. Comput. Intell.* **2008**, *122*, 209–229. [CrossRef]

72. Hanley, M.E.; Bouma, T.J.; Mossman, H.L. The Gathering Storm: Optimizing Management of Coastal Ecosystems in the Face of a Climate-Driven Threat. *Ann. Bot.* **2020**, *125*, 197–212. [CrossRef]
73. Norlin, B.; Assal, T. Data from: Mapping an Indicator Species of Sea Level Rise along the Forest-Marsh Ecotone. Available online: https://knb.ecoinformatics.org/submit/urn:uuid:bd1f89e8-3b73-4945-8d84-c17b5e7f10e3 (accessed on 23 July 2023).